# Comparative Evaluation of Chemically and Green-Synthesized Silica-Modified $CeO_2$ Nanostructures for Time-Dependent Room-Temperature Ammonia Sensing

## *Evaluación comparativa de nanoestructuras de $CeO_2$ modificadas con sílice, sintetizadas química y ecológicamente, para la detección de amoníaco a temperatura ambiente en función del tiempo*

## *Avaliação comparativa de nanoestruturas de $CeO_2$ modificadas com sílica, sintetizadas quimicamente e por métodos ecológicos, para detecção de amônia em função do tempo e à temperatura ambiente.*

*Danish Majeed [1], Syeda Sarah Zehra Zaidi [2], Syed Muhammad Mohsin [3], Muhammad Sajid Ali Asghar [4], Asad A. Zaidi [5] (*)*

Recibido: 12/01/2026 Aceptado: 27/03/2026

**Summary. -** Silica nanoparticles were synthesized via two distinct routes – a conventional chemical process and a sustainable green approach using sugarcane bagasse – and incorporated into cerium oxide ($CeO_2$) nanostructures for comparative evaluation as room-temperature ammonia ($NH_3$) gas sensors. The chemical route yielded silica by precipitating sodium silicate, whereas the green route extracted bio-silica from agricultural waste (sugarcane bagasse). Both silica types were integrated with $CeO_2$ through a precipitation/coating method to form silica–modified $CeO_2$ composite nanoparticles, which were fabricated into chemiresistive sensor devices. Structural characterization by scanning electron microscopy (SEM) revealed an elongated, rod-like $CeO_2$ morphology distributed in a silica-rich matrix, and energy-dispersive X-ray spectroscopy (EDS) confirmed the presence of Si, Ce, and O, indicating successful composite formation. Gas sensing tests demonstrated that all sensors responded to $NH_3$ at room temperature, with an initial rapid decrease in resistance upon $NH_3$ exposure. The gas response (defined as change in resistance ratio) reached over 600% within seconds of exposure for fresh sensors and progressively increased with continued exposure up to 10 min. After 15 min of continuous $NH_3$, however, the sensor response became negative (~–11%), suggesting surface saturation or irreversible adsorption of $NH_3$ on the active sites. These results suggest that sugarcane bagasse-derived silica can produce $NH_3$ response trends broadly comparable to chemically synthesized silica under the present experimental conditions. However, a full statistical comparison using multiple devices is still required to confirm equivalent performance. The incorporation of green-sourced silica thus provides an environmentally friendly pathway to high-performance, room-temperature gas sensors, though calibration and long-term stability tests are needed for further development.

***Keywords:*** *Silica nanoparticles; Green synthesis; Cerium oxide; Chemiresistive ammonia sensor; Room-temperature gas sensing*

(*) Corresponding author.

[1] PhD Scholar, Department of Materials Engineering, NED University of Engineering and Technology (Pakistan), Danish.majeed@neduet.edu.pk, ORCID iD: https://orcid.org/0009-0006-1005-8443

[2] Bachelor of Engineering (Materials), Department of Materials Engineering, NED University of Engineering and Technology (Pakistan), sara.zaidi@gmail.com. ORCID iD: https://orcid.org/0009-0005-1762-6530

[3] Bachelor of Engineering (Materials), Department of Materials Engineering, NED University of Engineering and Technology (Pakistan); mohsim.m@gmail.com, ORCID iD: https://orcid.org/0009-0006-0799-7925

[4] Associate Professor, Department of Materials Engineering, NED University of Engineering and Technology (Pakistan), smsajid@neduet.edu.pk, ORCID iD: https://orcid.org/0000-0002-4551-1299

[5] Professor, Department of Mechanical Engineering, Faculty of Engineering, Islamic University of Madinah (Saudi Arabia), ORCID iD: https://orcid.org/0000-0001-5457-5684

Memoria Investigaciones en Ingeniería, núm. 30 (2026). pp. 145-163
https://doi.org/10.36561/ING.30.10
ISSN 2301-1092 • ISSN (en línea) 2301-1106 – Universidad de Montevideo, Uruguay

***Resumen. -*** *Se sintetizaron nanopartículas de sílice mediante dos rutas distintas: un proceso químico convencional y un enfoque verde sostenible utilizando bagazo de caña de azúcar. Estas nanopartículas se incorporaron a nanoestructuras de óxido de cerio ($CeO_2$) para su evaluación comparativa como sensores de gas de amoníaco ($NH_3$) a temperatura ambiente. La ruta química produjo sílice mediante la precipitación de silicato de sodio, mientras que la ruta verde extrajo sílice biológica de residuos agrícolas (bagazo de caña de azúcar). Ambos tipos de sílice se integraron con $CeO_2$ mediante un método de precipitación/recubrimiento para formar nanopartículas compuestas de $CeO_2$ modificadas con sílice, las cuales se utilizaron para fabricar dispositivos sensores quimiorresistivos. La caracterización estructural mediante microscopía electrónica de barrido (SEM) reveló una morfología de $CeO_2$ alargada, en forma de varilla, distribuida en una matriz rica en sílice. La espectroscopia de rayos X de energía dispersiva (EDS) confirmó la presencia de Si, Ce y O, lo que indica la formación exitosa del compuesto. Las pruebas de detección de gases demostraron que todos los sensores respondieron al $NH_3$ a temperatura ambiente, con una rápida disminución inicial de la resistencia tras la exposición al $NH_3$. La respuesta al gas (definida como el cambio en la relación de resistencia) alcanzó más del 600 % en segundos para los sensores nuevos y aumentó progresivamente con la exposición continua hasta los 10 minutos. Sin embargo, después de 15 minutos de exposición continua al $NH_3$, la respuesta del sensor se volvió negativa (~–11 %), lo que sugiere saturación de la superficie o adsorción irreversible de $NH_3$ en los sitios activos. Estos resultados sugieren que la sílice derivada del bagazo de caña de azúcar puede producir tendencias de respuesta al $NH_3$ ampliamente comparables a las de la sílice sintetizada químicamente en las presentes condiciones experimentales. No obstante, aún se requiere una comparación estadística completa con múltiples dispositivos para confirmar un rendimiento equivalente. La incorporación de sílice de origen ecológico proporciona, por lo tanto, una vía respetuosa con el medio ambiente para obtener sensores de gas de alto rendimiento a temperatura ambiente, aunque se necesitan pruebas de calibración y estabilidad a largo plazo para su posterior desarrollo.*

***Palabras clave:*** *Nanopartículas de sílice; Síntesis verde; Óxido de cerio; Sensor quimiorresistivo de amoníaco; Detección de gases a temperatura ambiente.*

***Resumo*. -** *Nanopartículas de sílica foram sintetizadas por duas rotas distintas – um processo químico convencional e uma abordagem verde sustentável utilizando bagaço de cana-de-açúcar – e incorporadas em nanoestruturas de óxido de cério ($CeO_2$) para avaliação comparativa como sensores de gás amônia ($NH_3$) à temperatura ambiente. A rota química produziu sílica por precipitação de silicato de sódio, enquanto a rota verde extraiu biossílica de resíduos agrícolas (bagaço de cana-de-açúcar). Ambos os tipos de sílica foram integrados ao $CeO_2$ por meio de um método de precipitação/revestimento para formar nanopartículas compósitas de $CeO_2$ modificadas com sílica, que foram utilizadas na fabricação de dispositivos sensores quimiorresistivos. A caracterização estrutural por microscopia eletrônica de varredura (MEV) revelou uma morfologia alongada, em forma de bastonete, do $CeO_2$ distribuída em uma matriz rica em sílica, e a espectroscopia de raios X por dispersão de energia (EDS) confirmou a presença de Si, Ce e O, indicando a formação bem-sucedida do compósito. Os testes de detecção de gás demonstraram que todos os sensores responderam ao $NH_3$ à temperatura ambiente, com uma rápida diminuição inicial na resistência após a exposição ao $NH_3$. A resposta ao gás (definida como a variação na razão de resistência) atingiu mais de 600% em segundos após a exposição para sensores novos e aumentou progressivamente com a exposição contínua por até 10 minutos. Após 15 minutos de exposição contínua ao $NH_3$, no entanto, a resposta do sensor tornou-se negativa (aproximadamente -11%), sugerindo saturação da superfície ou adsorção irreversível de $NH_3$ nos sítios ativos. Esses resultados sugerem que a sílica derivada do bagaço de cana-de-açúcar pode produzir tendências de resposta ao $NH_3$ amplamente comparáveis à sílica sintetizada quimicamente nas condições experimentais atuais. No entanto, uma comparação estatística completa utilizando múltiplos dispositivos ainda é necessária para confirmar o desempenho equivalente. A incorporação de sílica de origem verde proporciona, portanto, um caminho ecologicamente correto para sensores de gás de alto desempenho que operam em temperatura ambiente, embora sejam necessários testes de calibração e estabilidade a longo prazo para o desenvolvimento futuro.*

***Palavras-chave:*** *Nanopartículas de sílica; Síntese verde; Óxido de cério; Sensor quimiorresistivo de amônia; Detecção de gases em temperatura ambiente*

**1. Introduction. -** Silica nanoparticles ($SiO_2$ NPs) are widely regarded for their high surface area, tunable size, thermal stability, and biocompatibility, making them versatile for applications in sensors, drug delivery, pollutant remediation, and catalysis [1], [2]. Traditionally, silica NPs are produced via chemical methods (e.g. sol–gel or Stöber processes) which offer controlled size and morphology but often involve harsh chemicals and energy-intensive steps [3]. These conventional processes raise environmental and safety concerns. In recent years, green synthesis approaches have gained momentum as sustainable alternatives [4], [5], [6]. Agricultural wastes such as rice husk, corn cob, and sugarcane bagasse have been identified as rich silica sources that can be processed into nanosilica, reducing waste and chemical usage [7], [8]. For instance, sugarcane bagasse ash can contain over 70 wt% silica [9], making it an attractive precursor for silica extraction. Utilizing such bio-derived silica not only diminishes the need for toxic reagents but also adds value to agro-industrial byproducts [10]. Recent studies have demonstrated feasible routes to synthesize silica nanoparticles from sugarcane bagasse and other plant wastes, underscoring the potential of green nanotechnology in materials engineering [11], [12], [13].

Cerium oxide ($CeO_2$) is a prominent metal oxide semiconductor with excellent redox activity and a high density of oxygen vacancies, properties that are highly beneficial for gas sensing applications [14]. These oxygen vacancies facilitate the adsorption and reaction of gas molecules on the surface, while $CeO_2$ has good thermal stability and environmental durability which are advantageous for sensor longevity [15]. $CeO_2$ is an n-type semiconductor that typically requires elevated operating temperatures to achieve sufficient surface reactivity; however, various strategies such as nanostructuring and doping have been employed to overcome its limitation of low room-temperature conductivity [16], [17]. In particular, modifying $CeO_2$ with secondary phases or dopants can dramatically enhance its gas response at lower temperatures by increasing surface area, creating heterojunctions, or introducing catalytic sites [18]. For example, incorporating noble metals or other oxides into $CeO_2$ has been shown to improve sensitivity and selectivity to target gases [19]. In one recent report, Ti-doped $CeO_2$ thin films exhibited a gas response of ~5910% to 250 ppm $NH_3$ at room temperature (compared to pristine $CeO_2$'s significantly lower response), with rapid response/recovery times of ~15 s [20]. These improvements were attributed to increased oxygen vacancy concentration and electronic modulation by the Ti dopant.

Another effective modification of $CeO_2$ is the addition of silica. Silica itself is electrically insulating, but when combined with metal oxides it can act as a high-surface-area framework that promotes dispersion of the active oxide phase and enhances gas diffusion through a porous network [21], [22]. Wang *et al.* demonstrated that a sensor using $CeO_2$ nanostructures modified with ~8 wt% $SiO_2$ achieved a remarkably high $NH_3$ response (~3244% to 80 ppm) at room temperature, far superior to pure $CeO_2$, along with a lower detection limit of 0.5 ppm [23]. The enhanced performance was attributed to the silica providing a larger effective surface and improved hydroxyl-mediated conductivity on the composite surface [24]. Silica additives can also stabilize the nanostructure and prevent particle agglomeration, thereby preserving active surface sites. Furthermore, silica's acid/base surface groups may interact with ammonia, influencing the sensor's electron transfer processes [25]. By fine-tuning the $SiO_2$ content, researchers have achieved sensors operable at room temperature with fast response and recovery and extended stability [26].

Accordingly, the objective of this study is to comparatively evaluate silica obtained via (i) a conventional chemical route and (ii) an agricultural waste–derived green route (sugarcane bagasse), after integration into silica-modified $CeO_2$ nanostructures for room-temperature $NH_3$ sensing. The work aims to (a) document the synthesis and fabrication workflow, (b) examine morphology and elemental composition using SEM/EDS, and (c) assess the time-dependent evolution of chemiresistive response under qualitative $NH_3$ exposure over 0–15 min. The emphasis is placed on comparative response trends and exposure-time effects relevant to practical room-temperature operation rather than ppm-calibrated sensitivity.

**2. Materials and Methods. -**

**2.1 Materials and Reagents. -** The silica sources and chemicals used in this work include: sodium silicate solution ($Na_2SiO_3$, for chemical silica synthesis), sugarcane bagasse (agricultural waste sourced locally, for green silica synthesis), hydrochloric acid (HCl, 2.5% aqueous solution), silver nitrate ($AgNO_3$), ethanol ($C_2H_5OH$), nitric acid ($HNO_3$), sodium hydroxide (NaOH), ammonium hydroxide ($NH_4OH$), and cerium(III) nitrate hexahydrate ($Ce(NO_3)_3 \cdot 6H_2O$). Distilled water was used in all synthesis and washing steps. All chemicals were of analytical grade and used as received.

**2.2 Silica Nanoparticle Synthesis by Chemical Route. -** Silica nanoparticles were synthesized using both a conventional chemical route and a green route based on agricultural waste in order to enable a comparative evaluation of their suitability for gas sensing applications. In the chemical synthesis approach, diluted sodium silicate solution

was added dropwise to 2.5% hydrochloric acid under continuous magnetic stirring at approximately 60 °C. The controlled neutralization process resulted in the formation of a cloudy, viscous silica gel due to the condensation of silicate species. The obtained gel was repeatedly washed with distilled water to remove residual chloride ions, which was confirmed by the absence of white precipitate upon addition of silver nitrate to the filtrate. The washed gel was then dried at 100 °C for 24 h, followed by calcination in air at 1000 °C for 1 h to obtain silica nanoparticles with enhanced thermal stability and structural integrity. The overall workflow of the chemical synthesis route is schematically shown in Figure I.

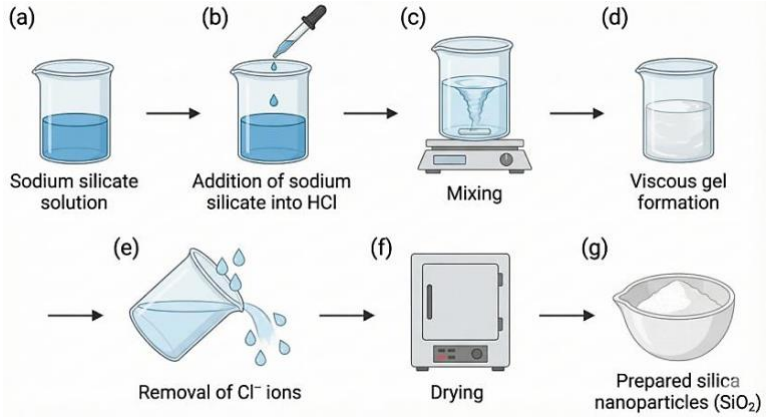


*Figure I.- Schematic illustration of the chemical-route synthesis of silica nanoparticles via acid precipitation, washing, drying, and calcination.*

The green synthesis route, composite preparation, and sensor fabrication steps are described separately in the following subsections to avoid repetition and improve clarity.

**2.3 Silica Nanoparticle Synthesis by Green Route. -** For the green synthesis route, silica was extracted from sugarcane bagasse, an agricultural by-product high in silica content [27]. The bagasse (fibrous sugarcane waste) was first sun-dried and cut into small pieces. It was then thoroughly washed with distilled water and soaked for 24 h to remove dirt and soluble impurities. After oven drying at 90 °C, the cleaned bagasse was subjected to acid leaching: the fibers were immersed in a 1 N HCl solution and heated in a water bath at ~75 °C for several hours. This step dissolves many metal impurities from the biomass [3]. The material was filtered, washed to neutrality, and dried again (90 °C). Next, the pretreated bagasse was transferred to a basic extraction step to dissolve its silica content. The dried fibers were boiled in 1 M NaOH solution (liquid-to-solid ratio ~10 mL $g^{-1}$) at 90 °C for 1 h, which converted the bio-silica into soluble sodium silicate. The hot mixture was filtered to remove residual biomass, yielding a sodium silicate solution. Silica was then precipitated from this solution by the addition of acid: concentrated $HNO_3$ was added dropwise to the filtrate under stirring until the pH lowered to ~8. At this point, the silicate condenses into silica particles, forming a suspension. A small amount of ethanol (~20 mL) was also added to promote particle formation. The suspension was continuously stirred, then left overnight. The silica product was collected by centrifugation at ~4000 rpm for 45 min, washed repeatedly with distilled water, and dried at 90 °C. A final calcination at 600 °C for 30 min was applied to obtain purified silica nanoparticles. Figure II summarizes the green synthesis steps.

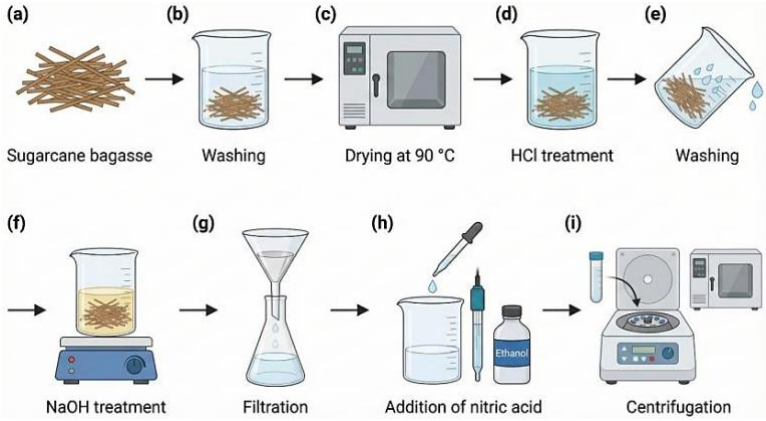


*Figure II.- Schematic workflow for green synthesis of $SiO_2$ nanoparticles from sugarcane bagasse via acid leaching, alkaline extraction, and acid precipitation.*

Both synthesis methods yielded fine white silica powders. The chemically synthesized silica had a yield of approximately 1.5–2 g from the starting solution volumes, whereas the green route yield depended on ash content (bagasse ash after acid treatment yielded ~20–25% silica by weight). The green synthesis is notably less toxic and aligns with sustainable practices by utilizing a renewable waste resource.

**2.4 Preparation of Silica–Modified $CeO_2$ Nanostructures. -** Silica-modified ceria nanostructures were prepared via an in situ precipitation of $CeO_2$ onto the silica nanoparticles. In a typical procedure, 6 g of the prepared silica nanoparticles (from either route) were dispersed in 100 mL of distilled water. The dispersion was ultrasonicated for 30 minutes to ensure a uniform suspension of silica particles (which serve as a substrate or template for $CeO_2$ growth). In parallel, 2.17 g of cerium (III) nitrate hexahydrate ($Ce(NO_3)_3 \cdot 6H_2O$) was dissolved in 50 mL of distilled water to form a $Ce^{3+}$ precursor solution. This cerium nitrate solution was then slowly added to the silica suspension under constant magnetic stirring. After 15 minutes of mixing, ammonium hydroxide ($NH_4OH$, ~28% solution) was added dropwise to the mixture until the pH reached approximately 10–11. The addition of $NH_4OH$ precipitates cerium as cerium hydroxide, which subsequently forms cerium oxide (ceria) in the presence of $OH^-$. The reaction was maintained at ~80 °C with continuous stirring for 2 hours to allow $CeO_2$ nanoparticles to nucleate and coat onto the silica surfaces. The appearance of a homogenous light yellow or off-white suspension indicated the formation of $CeO_2$ on $SiO_2$. The composite product was collected by centrifugation at 10,000 rpm for 10 minutes, then washed thoroughly with distilled water to remove any residual ions (e.g., $NH_4^+$, $NO_3^-$). The collected silica–ceria composite was dried in an oven at 80 °C for 12 hours. This drying step yields a powder comprising silica nanoparticles decorated with cerium oxide (denoted $CeO_2$–$SiO_2$ nanostructures). Figure III provides a stepwise illustration of the composite synthesis.

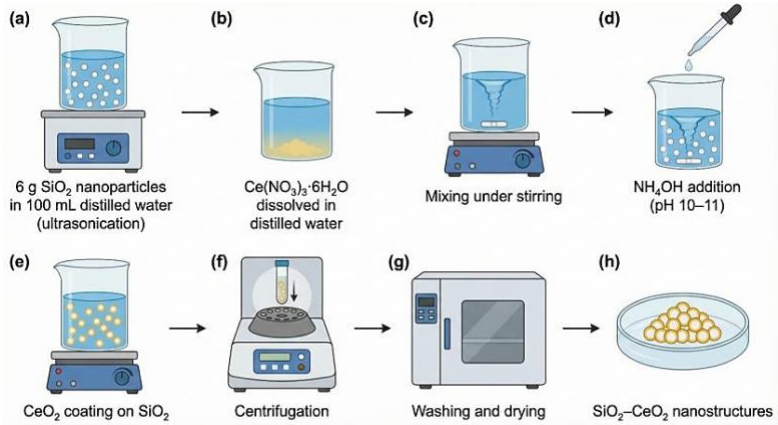


*Figure III.- Schematic of $CeO_2$–$SiO_2$ composite formation via precipitation/coating of ceria onto dispersed silica nanoparticles.*

In this synthesis, silica (from either source) plays the role of a high-surface-area scaffold. The precipitation of $CeO_2$ in the presence of dispersed silica promotes the formation of a **composite** rather than separate $CeO_2$ particles. Prior studies on similar systems have reported core–shell type structures where silica cores are coated with ceria shells [27], [28]. Our approach is expected to produce a network of $CeO_2$ nanocrystallites attached to silica surfaces, which can increase the effective interface with gas molecules during sensing [29].

**2.5 Sensor Fabrication and Electrical Measurements. -** A chemiresistive gas sensor device was fabricated using the silica–modified $CeO_2$ composite as the active material. The sensing element was prepared on a small glass substrate (approximately 2 × 2 cm). Prior to coating, the glass substrate was cleaned ultrasonically in ethanol and acetone (10 min each) and dried at 90 °C. Interdigitated electrodes were then formed on the glass surface to allow electrical contact to the sensor material. To do this, a thin conductive layer was applied using silver and gold pastes: first, a silver paste was painted as a seed layer for good adhesion, defining two opposite electrode pads. Then a layer of gold paste was applied over the silver tracks to provide a chemically inert, highly conductive electrode surface. The electrode pattern was dried and cured by heating at 90 °C for several hours, ensuring the metal contacts were well-adhered. Fine platinum wires were attached to the electrode pads (using additional silver paste) to serve as lead-out connections.

To prepare the sensing film, the dried $CeO_2$–$SiO_2$ composite powder was blended with a small amount of poly(vinyl alcohol) (PVA) as a binder. Specifically, PVA was dissolved in ethanol to create a viscous solution, and the silica–ceria powder was gradually added to form a slurry. Additional PVA or ethanol was mixed in as needed to achieve a spreadable paste with uniform consistency. The PVA acts as a temporary binder to hold the nanoparticles together and

adhere them to the substrate; it will evaporate or decompose upon subsequent heating, leaving a porous ceramic film. The composite paste was then coated onto the area between the gold contact pads on the glass substrate, covering the electrode gap. This coating was done carefully to create a thin, even film. After air drying, the coated sensor was cured by heating at 400 °C for 2 hours in air. Although the general fabrication procedure was described, some device-level parameters were not measured, including exact electrode gap width, finger length/number, film thickness, active coated area, curing ramp rate, and contact-resistance stability. These parameters may affect the absolute resistance and response values, so the device data were interpreted as proof-of-concept results. This thermal treatment burns off the PVA binder and improves adhesion of the composite to the substrate, as well as potentially enhancing particle connectivity by slight sintering. The result was a robust, porous sensing layer of silica–modified $CeO_2$ bridging the gold electrodes. Figure IV shows the fabrication steps and assembled sensor device.

For gas sensing tests, the fabricated sensor was placed inside an airtight chamber of approximately 1 L volume. Figure V shows the measurement setup. To introduce ammonia, a known volume of aqueous ammonia solution (~25% $NH_3$ in water) was placed in a shallow dish inside the sealed chamber. The volatile $NH_3$ evaporates from the solution, quickly enriching the chamber atmosphere with ammonia vapor. (Note: this method provides an uncalibrated concentration of $NH_3$; the exposure in this study is qualitative, since no mass flow controller or precise ppm control was used – see *Limitations*). Upon introducing $NH_3$, the sensor's resistance in the ammonia environment ($R_{gas}$) was recorded continuously. The sensor was exposed to ammonia for a total of 15 minutes, and the response was monitored over this duration. At 5-minute intervals (0, 5, 10, 15 min), the chamber was briefly opened and then resealed (for instance, to refresh the vapor or simulate consecutive exposures), and the subsequent resistance behavior was measured. After 15 min, the chamber was opened to allow the ammonia to dissipate and the sensor to recover in fresh air. Because the chamber was opened and resealed at 5-minute intervals, the ammonia concentration and oxygen availability inside the chamber were not constant throughout the experiment. Each opening allowed partial gas exchange with ambient air, which may have changed the $NH_3$ level and refreshed oxygen on the sensor surface. Therefore, the response curves at 0, 5, 10, and 15 min should be interpreted as successive chamber-exposure intervals rather than a strictly controlled continuous $NH_3$ exposure history.

The gas response of the sensor is defined in percentage terms using the standard chemiresistive formula:

$$\text{Gas Response (\%)} = \frac{R_{\text{air}} - R_{\text{gas}}}{R_{\text{air}}} \times 100,$$

Where, Rair is the sensor resistance in air (baseline) and Rgas is the resistance in the target gas (here, $NH_3$) [9]. According to this definition, a decrease in resistance upon gas exposure (typical for an n-type oxide like $CeO_2$ in the presence of a reducing gas) yields a positive response percentage. Since this response calculation depends on the selected air baseline resistance, any baseline drift during prolonged exposure or incomplete recovery can strongly affect the calculated response value. Therefore, a change in response sign may occur if the baseline shifts, and it should not automatically be interpreted as a true inversion of the sensing mechanism. All response values reported were calculated with this formula. In our measurements, the sensor's real-time resistance changes were captured and later converted to response (%) versus time for analysis.

No external heating was applied to the sensor – all tests were conducted at room temperature (~25 °C). The humidity level was ambient (~50% RH) and was not specifically controlled. After each test, the chamber was purged and the sensor was allowed to recover in air; however, as discussed later, the 15-minute prolonged exposure led to behavior suggesting incomplete recovery.

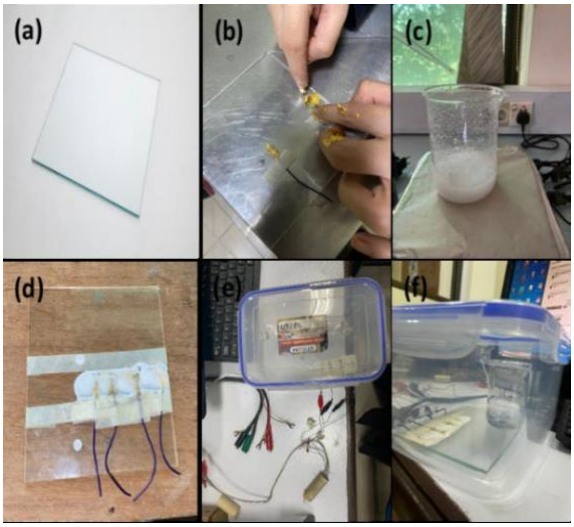


*Figure IV. Schematic representation of gas sensor fabrication using silica-modified $CeO_2$ nanostructures on a glass substrate.*

It should be noted that because the ammonia concentration in the chamber was not quantitatively measured (relying on evaporation from solution), the response data are interpreted qualitatively. The emphasis of this study is on comparing the *relative* sensor behavior (especially time-dependent characteristics and the effect of prolonged exposure) rather than on an exact sensitivity value to a known ppm. The performance of our sensor is also compared with literature reports to contextualize its sensitivity.

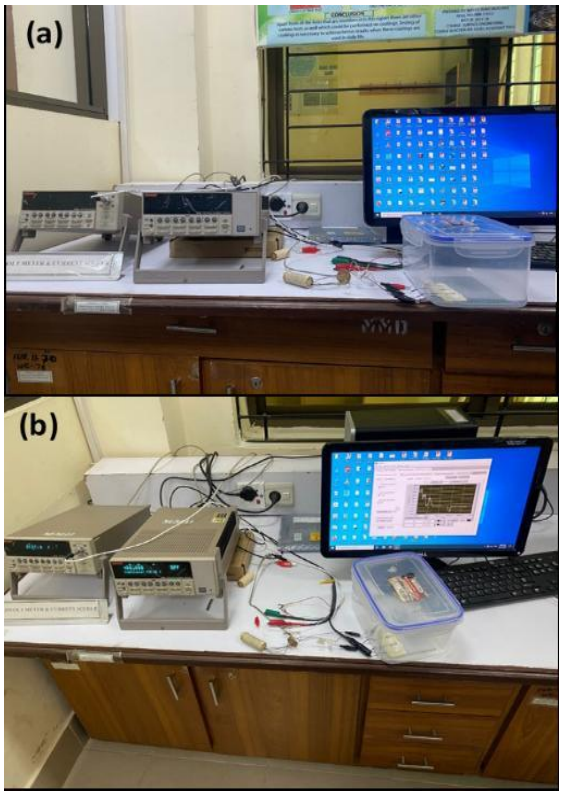


*Figure V. Schematic of the sealed-chamber setup used for room-temperature ammonia sensing* measurements.

**3. Results and Discussion. -**

**3.1 SEM Analysis of Silica–Ceria Nanostructures. -** The morphology of the silica–modified $CeO_2$ nanostructures was examined by SEM. Representative SEM micrographs at different magnifications are shown in Figure VI.

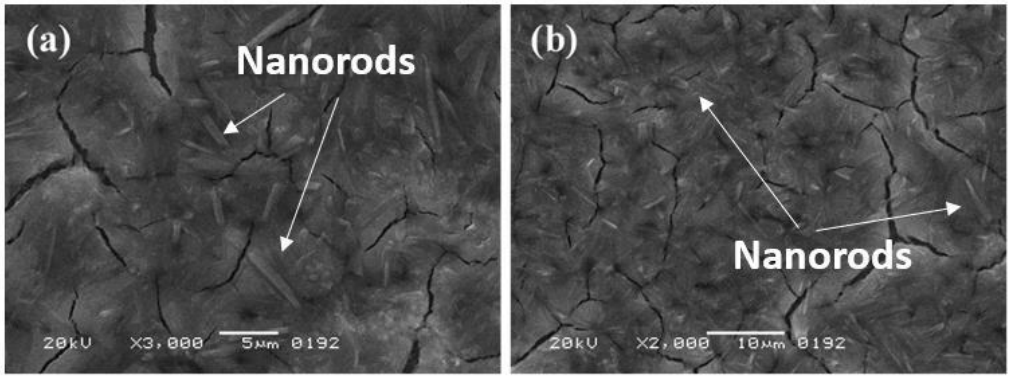


*Figure VI. SEM micrographs of silica-modified $CeO_2$ nanostructures at different magnifications.*

Comparing our SEM observations with literature, we note that Kitsou *et al*. (2019) achieved core–shell ZnO@$SiO_2$ particles where silica served as a smooth nanoscopic template for uniform oxide deposition [14]. In our case, the ceria does not form discrete core–shell particles but rather continuous ceria-rich rods embedded in silica. This structure resembles findings by Vaizoğullar *et al*. (2016), who prepared $SiO_2$@$CeO_2$ core–shell nanoparticles and observed a silica-rich composition with ceria coating the silica surfaces [30]. Our sample's rod-like, intergrown morphology may result from the high loading of $CeO_2$ relative to silica (6 g silica vs ~2 g Ce precursor used). As ceria nucleates and grows, particles coalesce into larger rods, possibly with silica particles decorating or interspersed within these rods. Some cracks or irregular voids are visible in the SEM images, which could be attributed to stresses during the high-temperature curing or calcination process. Thermal history (e.g. rapid drying or the 400 °C curing step) can induce fracturing in the deposited film, as noted in other nanoparticle-based coatings [31]. Despite these fractures, the SEM images show an interconnected composite morphology. However, based on the EDS results, the material should be described more carefully as a silica-rich structure containing dispersed Ce-containing oxide regions, rather than as a fully ceria-rich network.

The elongated ceria structures observed here are known to enhance gas sensing performance by offering a high surface-to-volume ratio and facilitating charge transport along the length of the rods [10]. One study on porous ceria nanorods (Tian *et al*., 2015) noted their high catalytic activity and robust performance, attributing it to the rod morphology providing abundant active sites and pathways for reactant diffusion [20]. In our composite, the silica component further contributes by increasing porosity and stability. Thus, the SEM results confirm that we have successfully created a nanostructured $CeO_2$–$SiO_2$ material with characteristics favorable for gas sensing: nanoscale rods, extensive surface area, and a percolating network structure. It should be noted that the rod-like features observed at the applied SEM magnifications correspond to micron-scale elongated structures, likely formed by the aggregation of nanoscale $CeO_2$ crystallites.

**3.2 EDS Analysis and Composition. -** Energy-dispersive X-ray spectroscopy was used to verify the elemental composition of the silica–ceria composite. Figure VII shows the EDS spectrum of a representative sample region.

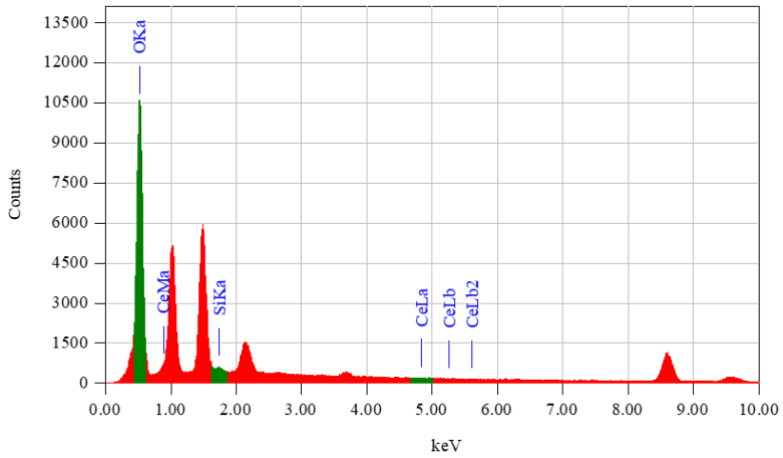


*Figure VII. EDS spectrum of silica-modified $CeO_2$ nanostructures showing the presence of Si, Ce, and O.*

The EDS results should be interpreted as semi-quantitative local compositional data from the analyzed surface region. The measurement was performed at 20.0 kV with a probe current of 1 nA, and the calculated weight percentages may vary with selected area, surface roughness, sample thickness, and local particle distribution. Therefore, the EDS values were used mainly to confirm the presence of Si, Ce, and O, rather than to define the exact bulk composition of the composite. The silica-rich composition has important implications for gas sensing. A high $SiO_2$ content contributes a large surface area and porous structure, as silica generally forms porous networks. The Ce-containing oxide phase was present in a lower amount than silica and was likely distributed as dispersed regions, clusters, or partial coating on the silica-rich matrix. Therefore, the role of $CeO_2$ in sensing was discussed as the contribution of accessible Ce-containing active sites, while silica was considered mainly as the supporting matrix. Vaizoğullar *et al*. (2016) observed that in $SiO_2$@$CeO_2$ core–shell nanoparticles with similarly low Ce content, the configuration enhanced adsorption capabilities – in their case for Hg(II) removal – due to the silica providing a high-surface-area support for the active $CeO_2$ phase. By analogy, our composite's elemental makeup (low Ce, high $SiO_2$) points to a design wherein $SiO_2$ is the structural scaffold and $CeO_2$ provides the reactive sites for ammonia sensing. This division of roles can be advantageous: silica ensures a stable, porous film, and ceria, despite its smaller fraction, can strongly influence sensor response due to its catalytic redox interactions with gases [24].

Furthermore, the presence of oxygen (50+ wt%) in the EDS confirms that the material consists of oxides (as expected: $SiO_2$ and $CeO_2$). No metallic Ce or unoxidized silicon is detected, implying that during synthesis and curing, cerium precipitated as cerium oxide and the silica remained in oxide form. The EDS result thus corroborates that the intended composite ($SiO_2$ and $CeO_2$) was obtained. We acknowledge that a precise phase identification (e.g. crystalline phase of $CeO_2$) would require X-ray diffraction (XRD). In this study, XRD was not performed; however, literature and the synthesis conditions strongly suggest that the cerium is present as $CeO_2$ (fluorite structure), likely nanocrystalline or possibly amorphous if insufficiently crystallized at 80 °C. The decision to focus on SEM/EDS for composition was made to prioritize understanding the sensor's functional performance. Despite the lack of XRD confirmation, the effective gas sensing behavior (discussed below) provides indirect evidence of active $CeO_2$ presence, since pure silica is inert to ammonia under these conditions. This revised interpretation reconciles the SEM and EDS observations: the composite was not treated as a ceria-rich percolating network, but as a silica-rich material containing Ce-containing oxide sites that may participate in $NH_3$ sensing.

**3.3 Gas Sensing Mechanism (Chemiresistive Response). -** Before discussing the experimental gas response results, we briefly outline the sensing mechanism for n-type semiconducting oxides like $CeO_2$. In ambient air, oxygen molecules adsorb onto the surface of $CeO_2$ and capture electrons from the material's conduction band, forming chemisorbed oxygen species ($O_2^-$, $O^-$, $O^{2-}$) [9]. This creates an electron depletion layer at the surface, raising the sensor's resistance in air (Rair). When the sensor is exposed to a reducing gas such as $NH_3$, the gas molecules react with these adsorbed oxygen ions. For ammonia, a representative surface reaction can be written as:

$$2NH_3(gas) + 3O^-(ads) \rightarrow N_2(gas) + 3H_2O(gas) + 3e^-,$$

which indicates that $NH_3$ donates electrons back to the oxide by consuming surface oxygen species. The product $N_2$ and $H_2O$ desorb, and the released electrons return to the $CeO_2$, reducing the depletion layer and thereby decreasing the sensor's resistance. Thus, upon $NH_3$ exposure, an n-type oxide sensor typically shows a drop in resistance, which we quantify as a positive gas response (%) as per the earlier formula. When the $NH_3$ is removed and air is reintroduced, oxygen readsorption can restore the initial conditions (electrons re-trapped by $O_2$, resistance rises back to baseline), ideally regenerating the sensor.

In our silica–$CeO_2$ composite, the same fundamental mechanism applies, but the silica matrix may influence the process by affecting how gases diffuse and how electrons percolate. The silica itself is insulating, so the conductive path is primarily through the ceria domains. However, silica can adsorb moisture and surface hydroxyls which might interact with $NH_3$ (for example, $NH_3$ can temporarily bind to silanol groups). This could introduce additional surface reactions or delay the recovery as discussed later. Nonetheless, the dominant sensing action is expected from the $CeO_2$ sites.

We next present the sensor response results at different exposure times. To reiterate, all measurements were done at room temperature with an unquantified but repeatable $NH_3$ dose (from evaporating ammonia solution). The baseline resistance in air for our devices was on the order of a few MΩ. Upon $NH_3$ introduction, the resistance dropped markedly. We calculated the gas response (%) over time for each exposure interval (0, 5, 10, 15 min exposures). The dynamic response curves are shown in Figures VIII–XI, and key features are discussed below. It is important to note that the 0, 5, 10, and 15 min response curves do not represent a fully controlled continuous exposure experiment. Since

the chamber was opened and resealed between intervals, gas composition, ammonia vapor concentration, and oxygen availability may have changed during the test. Therefore, the following discussion focuses on qualitative time-dependent response behavior under the present chamber protocol, rather than controlled kinetic analysis.

**3.3.1 Sensor Response at Initial $NH_3$ Exposure (0 minutes). -** "0 minutes" corresponds to the sensor's immediate reaction as ammonia is introduced (the first exposure, effectively within the first few seconds of sensing). Figure VIII displays the response curve at this initial exposure.

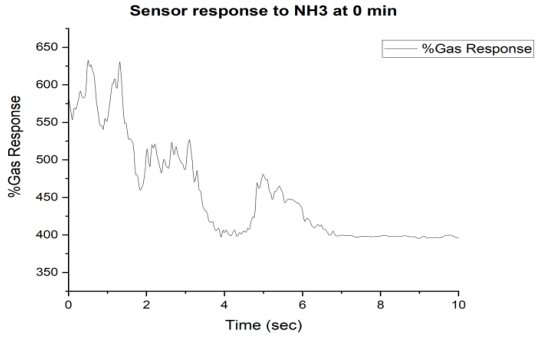


*Figure VIII. Dynamic $NH_3$ response of the sensor at 0 min exposure time.*

Following the peak, the sensor's response begins to decline gradually. In Figure VIII, after the first ~2 s spike, the % response drops and stabilizes around ~390–400% by 10 s. This decline is attributed to a partial recovery or saturation effect – as ammonia initially floods the surface, a maximum number of reaction sites are consumed (peak response), and subsequently the system reaches a balance where some $NH_3$ may desorb or the reaction by-products (e.g. water) start to occupy sites, causing a slight rebound in resistance [32]. A minor secondary rise ("bump") around 5–6 s can be seen, which could indicate a two-step adsorption process or a delayed reaction on deeper sites. By ~10 s, the curve has leveled off, implying that most accessible sites have reacted and the sensor is in a quasi-steady state with that ammonia dose. Importantly, when the chamber was later opened (to simulate a fresh exposure at 5 min, as described next), the sensor resistance returned close to baseline (with air flush), confirming that the interaction at this stage was largely reversible.

Overall, the initial exposure demonstrates that both chemically synthesized silica and green-synthesized silica composites can detect $NH_3$ strongly at room temperature. The magnitude of the response (hundreds of percent) is on par with or exceeds many conventional metal-oxide sensors at much higher operating temperatures [33]. The rapid response (sub-second rise) is a favorable attribute for real-time monitoring. This performance can be attributed to the composite's high surface area and the efficient catalytic reaction of $NH_3$ with chemisorbed oxygen on $CeO_2$. The presence of silica likely enhances the dispersion of $CeO_2$ and keeps the nanostructure porous, allowing $NH_3$ to penetrate and reach active sites quickly. We also note that at this initial stage, the sensor had not been "aged" by prior exposure, which often yields the highest response. Subsequent exposures (without thorough reoxidation in between) can show modified behavior, as we observed.

**3.3.2 Sensor Response after 5 Minutes of $NH_3$ Exposure. -** After the first exposure, the chamber was resealed with a continued $NH_3$ source for 5 minutes. We define the "5 min" response as the sensor's behavior when it is exposed to $NH_3$ that has been in the chamber for 5 minutes (a somewhat refreshed $NH_3$ environment, though not a fully desorbed baseline). Figure IX shows the dynamic response curve at the 5-minute mark.

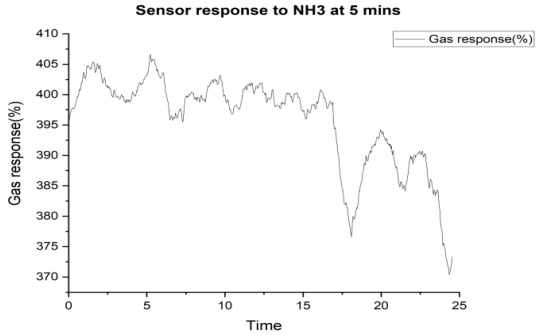


*Figure IX. Dynamic $NH_3$ response of the sensor at 5 min exposure time.*

Interestingly, the 5-min response curve shows a more complex transient. Around 10–15 s, there is an abrupt dip: the response drops from ~450% to ~375%, then partially recovers to ~395%, and then gradually falls to ~370% by ~25 s. This oscillatory behavior suggests a dynamic competition between adsorption and desorption processes. The momentary drop at ~15 s could indicate that a fraction of $NH_3$ desorbed or that a second-stage reaction (perhaps oxidation of intermediate species) occurred, momentarily increasing resistance. The subsequent partial recovery implies that $NH_3$ readsorbed on freed sites, and finally the downward drift toward 25 s signals a slow approach to equilibrium or slight poisoning. Essentially, by 5 minutes exposure, the sensor is entering a regime of saturation and partial regeneration simultaneously – ammonia molecules continue to interact, but the surface is not as uniformly receptive as at time zero. Similar kinetic behaviors (initial spike followed by dip and plateau) have been reported for other porous sensors under continuous gas flow, where the fast initial reaction is followed by slower diffusion-limited or desorption-limited stages.

From a sensing standpoint, the 5 min exposure still yields a high response (~370% sustained), which confirms that the sensor remains highly sensitive even after being subjected to $NH_3$ for a prolonged period. However, the reduction in peak and the fluctuations indicate that the sensor's surface is beginning to saturate. This is an important observation for practical use: it suggests that while short bursts of $NH_3$ can be detected with extreme sensitivity, continuous exposure will reduce the incremental response. The sensor is likely desorbing some ammonia during the exposure (hence the dip and partial recovery), which is a form of self-purging. This behavior is beneficial in that it prevents total saturation within minutes, but it also means the sensor response at long times may not remain at the initial high level.

**3.3.3 Sensor Response after 10 Minutes of $NH_3$ Exposure. -** Continuing the exposure further, the sensor behavior at 10 minutes in ammonia was recorded. Figure X presents the response curve after 10 min of continuous $NH_3$ environment.

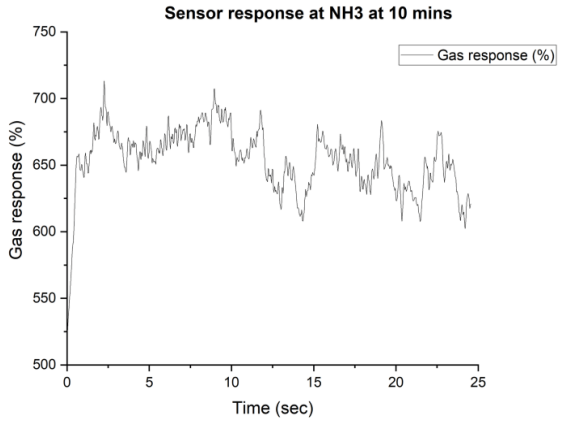


*Figure X. Dynamic $NH_3$ response of the sensor at 10 min exposure time.*

Following the peak, from ~3 s onward, the response does not simply decay; instead, it oscillates between about 660% and 700% for an extended period (several seconds). This quasi-steady oscillation indicates a dynamic equilibrium where ammonia adsorption and reaction are balanced by desorption and possibly oxygen re-adsorption in pockets of the sensor [34]. The porous structure likely allows $NH_3$ to diffuse in and out at different rates, causing fluctuations. Tong *et al.* (2017) observed analogous oscillatory response in a highly porous $H_2S$ sensor, attributing it to the interplay of gas diffusion and reaction kinetics in nanochannels [21]. In our case, the silica–ceria network might have regions that momentarily saturate and then refresh as $NH_3$ penetrates deeper. The presence of silica could also buffer moisture produced by ammonia oxidation, releasing it intermittently and affecting conductivity slightly.

After ~15 s, the sensor's response in Figure X begins a gradual decline, dropping to around 610% by 25 s. This downward trend suggests the onset of more significant surface saturation – many of the active sites are occupied by reaction products or a stable layer of adsorbed ammonia species, and the sensor cannot sustain the earlier high conductance. Nonetheless, even at 25 s, the response (~610%) is far above the baseline (0%). Compared to the earlier exposures, the 10-min case shows the sensor reaching its *highest* sensitivity (initially) and then showing signs of leveling off at a high response value. The fact that the sensor can still exceed 600% response at 10 min indicates a time-dependent activation: prolonged exposure appears to have activated additional sites or reduced the material (increasing $Ce^{3+}$ concentration), thus temporarily boosting sensitivity. Such behavior – an increase in response with

longer exposure – has been reported for some metal oxide sensors, often due to gradual temperature equilibration or surface restructuring in continuous gas. In our room-temperature case, it could be chemical restructuring (e.g., formation of ammonium species on the surface that facilitate more electron transfer).

This 10-min result highlights that the sensor's response is not static; instead, it evolves with prolonged gas interaction. Practically, this could manifest as a drift in sensor readings over time if $NH_3$ remains present. Initially, the readings might climb (super-sensitivity), then oscillate, and slowly decline as equilibrium is reached. For a sensing application, one would ideally calibrate the sensor at a fixed exposure duration or dynamic flow to avoid misinterpreting these time-dependent changes as concentration changes. In our experiments, since the concentration wasn't fixed, we interpret these results qualitatively: the composite sensor retains high responsiveness up to 10 minutes, but the reaction kinetics and surface coverage become increasingly complex.

**3.3.4 Sensor Response after 15 Minutes of $NH_3$ Exposure. -** After a continuous exposure of 15 minutes to ammonia, a striking change in sensor behavior was observed. Figure XI shows the response curve at the 15-min mark. It should be noted that the response value was calculated using the air baseline resistance. If this baseline resistance changed during the prolonged test, or if the sensor did not fully recover before the next measurement interval, the calculated response could become negative even without a true reversal of the $NH_3$ sensing mechanism. Therefore, the negative response at 15 min should be interpreted cautiously.

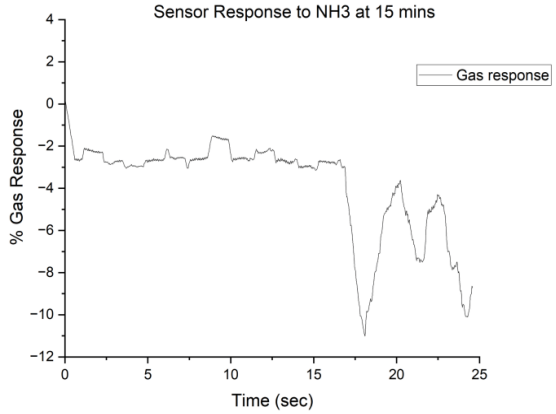


*Figure XI. Dynamic $NH_3$ response of the sensor at 15 min exposure time showing response inversion.*

This anomalous negative response may indicate sensor saturation or overload; however, it cannot be assigned only to this mechanism because the $NH_3$ concentration and humidity were not controlled during the test. Baseline drift, changes in chamber atmosphere, moisture effects from aqueous ammonia, or measurement-related artifacts may also have contributed to the negative response. By 15 minutes, it appears that the sensor surface has accumulated a high coverage of adsorbed species (likely $NH_3$-derived intermediates or reaction products like ammonium salts or strongly bound oxygen complexes) that fundamentally alter the material's conduction. One interpretation is that the prolonged $NH_3$ exposure caused an accumulation of electrons in the material that shifted the baseline (essentially reducing the oxide significantly). If the sensor baseline resistance had dropped over time (due to partial reduction), then upon final exposure, introducing $NH_3$ might no longer produce a drop in resistance – instead, if oxygen was completely depleted from the surface, $NH_3$ might actually start donating electrons that *overpopulate* the conduction band, leading to a temporary increase in resistance via complex mechanisms (such as formation of surface states that scatter electrons). Another simpler explanation is surface saturation: all adsorption sites (oxygen vacancies, etc.) are occupied, and additional $NH_3$ cannot react with $O^{2-}$ (because few are left); instead, $NH_3$ may physically adsorb as a neutral or insulating layer, increasing resistance or blocking current paths [35]. The relatively flat response for the first ~10 s suggests the sensor was fully saturated – the response hovered near 0% (no change). Then, the continuous decline to –11% by 25 s could indicate a slow poisoning effect, where the prolonged presence of $NH_3$ (or perhaps accumulation of by-products like ammonia-derived surface complexes) inverted the sensor's response. Essentially, the sensor's behavior degraded after too long an exposure, consistent with reversible damage or inhibition of the normal sensing reaction. Similar findings have been noted by Mei *et al*. (2024) for prolonged exposure of certain gas sensors, where signal saturation or even inversion was observed when the target gas was not removed, due to complete consumption of surface oxygen and accumulation of reducing species [17]. Likewise, Takte *et al*. (2023) reported that extended exposure to ammonia could lead to formation of stable surface residues (e.g., ammonium carbonates or amides) on ceria-based sensors, which alter the material's electronic structure and impede the usual sensing mechanism [18].

Therefore, the negative response observed at 15 min should be treated as a possible sign of surface saturation or altered surface condition, rather than as confirmed evidence of sensor poisoning. Further controlled experiments using fixed $NH_3$ concentration, controlled humidity, repeated cycles, and baseline stability checks are required to confirm the cause of this response inversion.

It is important to clarify that once the sensor is in this state, simply purging with air may not immediately restore the original baseline. Indeed, after the 15-min test, our sensor showed difficulty returning to the exact initial resistance, indicating that some $NH_3$ or reaction product remained bound (irreversible adsorption). In practical terms, this means the sensor would require re-oxidation (for example, heating or a long ambient recovery) to fully reset after such a prolonged $NH_3$ exposure. For shorter exposures (0–10 min), the sensor largely recovered after air purging, but the 15 min case crossed a threshold into saturation. This finding underscores a limitation for using such sensors in high or continuous ammonia environments: one must either periodically recondition the sensor or interpret the decreasing signal as an indicator of prolonged exposure (rather than misinterpreting it as lower gas concentration).

In summary, the time-dependent gas response measurements reveal a progression: (i) an initially high and fast response (0 min), (ii) slight moderation and kinetic complexity at 5 min, (iii) reactivation and oscillatory equilibrium at 10 min, and (iv) saturation and response inversion at 15 min. This progression can be understood as the sensor material transitioning from an ideal surface with abundant reactive oxygen (at start) to a surface that is progressively reduced and saturated by ammonia. The negative response at 15 min is a clear sign of sensor saturation, where additional reducing gas no longer yields a typical n-type response.

Notably, such behavior is rarely reported in short laboratory tests but is crucial for real-world sensing scenarios. It suggests that for long-term monitoring, either periodic sensor regeneration (e.g., exposure to clean air or mild heating to desorb residues) is necessary, or one should limit the sensor's exposure time within a regime that avoids complete saturation. The use of silica in our composite might contribute to the saturation effect as well – silica surfaces could hold $NH_3$ or moisture strongly over time, hindering the replenishment of oxygen on $CeO_2$. In future designs, optimizing the silica content or adding catalytic additives (e.g., Pt, as often done with MOX sensors [9]) could help mitigate such saturation.

Comparatively, the performance of our sensor in the initial phases is highly encouraging. Achieving >600% response to ammonia at room temperature with a simple composite (and without noble metal catalysts) is a testament to the synergy of the $CeO_2$–$SiO_2$ system. Other recent developments, like Fe/Cd co-doped $CeO_2$, have reported even higher responses (e.g. a response ~5004 to 200 ppm $NH_3$) but required careful doping strategies. Our approach uses a green-synthesized silica to achieve substantial sensitivity, highlighting that even *bio-silica* can serve effectively in sensor composites. Under the present test conditions, the sensors prepared using chemical-route silica and green-route silica showed broadly similar response patterns. However, because the number of tested devices was limited, these results should be considered a feasibility demonstration rather than proof of equivalent performance. This is an important validation of the green silica's applicability. Any slight variations (such as perhaps surface area differences) could influence absolute response magnitudes, but within the qualitative scope of our study, both routes produced sensors that behave similarly. The comparison between chemically synthesized silica and green-synthesized silica should be considered preliminary. In this study, the response trends were compared under the same general fabrication and testing procedure, but a rigorous statistical comparison was not performed. Multiple sensors from each group, baseline resistance distribution, mean response values, standard deviation, and significance testing would be required to confirm whether both routes truly show equivalent performance.

Overall, the results demonstrate that silica–modified $CeO_2$ composites are capable of detecting ammonia at room temperature with high sensitivity. The time-evolution of the sensor response provides insight into the surface chemistry dynamics, and the eventual saturation warns of the need for calibrated operation. These findings contribute to the understanding of how integrating a sustainable silica source with a metal oxide can yield a functional sensor, while also pointing out the practical considerations for deploying such sensors in real conditions.

**4. Limitations of the Study. -** While the silica–ceria $NH_3$ sensor demonstrated promising performance, several limitations must be acknowledged:

- **Qualitative Gas Exposure:** The ammonia sensing tests in this study were conducted without a calibrated gas flow or known concentration. $NH_3$ was introduced by evaporation from a solution in a sealed chamber, which provides an unquantified concentration of ammonia. Consequently, we report response trends (percentage change in resistance) rather than sensitivity to a specific ppm level. The lack of precise concentration control

means we cannot construct a response vs. concentration curve or determine a limit of detection. In practical sensor development, a controlled test (using mass flow controllers to mix known ppm of $NH_3$ in air) is essential for calibration. Our results are thus qualitative – they confirm ammonia detection and relative response behavior, but do not yield data on minimum detectable concentration or linear range. Future work should include quantitative gas dosing to fully evaluate the sensor's sensitivity and selectivity.

- **Absence of Structural Phase Confirmation (XRD):** We did not perform X-ray diffraction analysis on the synthesized composites. As a result, the crystallographic structure and phase purity of $CeO_2$ in the composite were not directly confirmed. We assumed the formation of $CeO_2$ based on the precursor and conditions, and the EDS elemental analysis supports this. However, without XRD we cannot ascertain the crystallite size or whether any Ce silicate phases formed at the interface. The decision to omit XRD was made to focus on functional testing and because the silica is largely amorphous (which would produce a broad background in XRD). This is a limitation because crystallinity can affect gas sensing properties. In future studies, performing XRD would be useful to correlate the sensor performance with any phase information (e.g., confirming nanoscale $CeO_2$ fluorite structure). Nonetheless, the significant sensor response observed suggests that the active $CeO_2$ phase was present and operative. In addition, SEM and EDS alone could not confirm the $CeO_2$ crystalline phase, $Ce^{3+}/Ce^{4+}$ ratio, oxygen vacancy concentration, or silica–ceria interface chemistry. Further characterization such as XRD, XPS, BET surface area analysis, and interface-focused analysis is important to fully confirm the structure and sensing mechanism of the composite. BET surface area and pore-size analysis were not performed in this study. Therefore, the role of silica in increasing surface area, porosity, and gas diffusion was not directly confirmed by experimental surface area data. In this manuscript, these effects were discussed only as possible contributions based on the known behavior of silica-containing oxide composites and the observed SEM morphology. Future work should include BET and pore-size analysis to directly relate surface area and porosity to $NH_3$ sensing performance.

- **Surface Saturation and Recovery:** As observed in the 15 min exposure test, the sensor can become saturated by ammonia, leading to an inverted (negative) response and incomplete recovery. This indicates a limitation in long-term stability under continuous exposure. The irreversible adsorption of $NH_3$ or its by-products on the sensor surface can degrade performance and require intervention (e.g., cleaning or reactivation by heating in air). In a practical scenario, sensors would likely be exposed to fluctuating concentrations rather than constant high levels of $NH_3$ for 15 minutes, but the result highlights the need for either periodic regeneration or operational protocols (like exposure cycles within a safe duration). Our study did not investigate the long-term repeatability or stability beyond the single sequence of exposures. It is possible that repeated exposure/recovery cycles could gradually change the baseline or response (sensor drift). This was not characterized here and remains as future work. In addition, because $NH_3$ concentration and humidity were not controlled, the negative response after prolonged exposure may also include the effects of baseline drift, moisture variation, chamber atmosphere changes, or measurement artifacts. The response calculation is also sensitive to the selected air baseline resistance; therefore, incomplete recovery or baseline drift during the test may have affected the calculated response values, including the negative response observed after 15 min.

- **Lack of Selectivity Tests:** We focused solely on ammonia sensing in this work. The selectivity of the silica–$CeO_2$ sensor towards $NH_3$ over other gases (like humidity, $CO_2$, ethanol, $NO_2$, etc.) was not evaluated. $CeO_2$ is known to also respond to other reducing gases (and to a lesser extent oxidizing gases), and the presence of silica might introduce sensitivity to moisture (due to hydrophilic silanol groups). Without selectivity data, it is uncertain how the sensor would perform in complex atmospheres. For instance, a real air environment with humidity could affect the baseline and response amplitude (water molecules can occupy sites or react with ammonia to form ammonium hydroxide on the surface). Future investigations should include tests with common interfering gases and varying humidity to determine the sensor's selectivity profile. Techniques such as surface functionalization or operating the sensor in pulsed mode (as some studies do) might be required to enhance selectivity. For room-temperature $NH_3$ sensing, humidity effects and cross-sensitivity to common gases are especially important. In this study, a humidity-response test and selectivity matrix against common interferents were not performed. Therefore, no claim is made regarding humidity tolerance or selective $NH_3$ detection in complex gas environments. Future work should include testing at different relative humidity levels and against common interfering gases such as $CO_2$, ethanol, $NO_2$, CO, and other volatile compounds to confirm practical selectivity.

- **Reproducibility and Sample Variability:** Due to resource constraints, we tested a limited number of sensor devices. The data presented are representative of the observed behavior, but we have not performed a

statistical analysis over many devices or multiple batches of materials. There may be variability in the silica produced by the green route (depending on bagasse source or processing) which could affect sensor performance consistency. Ensuring reproducible synthesis, especially for the green-silica, is a challenge – slight changes in bagasse composition or processing temperature could alter the surface area or impurity content of the silica. Our results show feasibility, but scalability would require careful standardization of the green synthesis protocol. In addition, device-to-device variability, repeated exposure–recovery cycles, recovery time after each $NH_3$ exposure, and aging stability were not evaluated in this study. Therefore, the reported sensing results should be considered initial proof-of-concept behavior under the tested conditions. Further work should include multiple devices, cyclic response testing, recovery-time measurement, and long-term aging studies to confirm reproducibility and practical stability.

In summary, while the study successfully demonstrates a proof-of-concept sensor using green-sourced silica, the above limitations suggest caution. The device is at a prototype stage: it works under the conditions tested, but further refinement and characterization (quantitative calibration, selectivity, stability) are needed before it could be deployed as a reliable $NH_3$ sensor. Addressing these limitations will be important for future research. For instance, performing calibrated tests could reveal the actual sensitivity (e.g., what ppm gives a 100% response, etc.) and whether the green-silica sensor meets required detection limits (typical safety thresholds for $NH_3$ are tens of ppm). Despite these limitations, the study provides valuable insights – particularly the observation of time-dependent response evolution – that can guide the development of robust gas sensors using sustainable materials.

**5. Conclusions. -** In this work, we synthesized silica nanoparticles via two routes – a conventional chemical method and an agricultural waste-derived green method – and utilized both types of silica to create silica–modified $CeO_2$ nanostructures for ammonia gas sensing at room temperature. The study was framed to compare the applicability of chemically produced versus "green" silica in functional sensor devices. Key conclusions are as follows:

- Sustainable Silica Synthesis: Sugarcane bagasse, an abundant agricultural by-product, was successfully converted into nanosilica using a simple acid/base extraction approach. The green-sourced silica was obtained after acid leaching and calcination, and its successful incorporation into the sensor demonstrates the feasibility of using agricultural waste-derived silica in silica-modified $CeO_2$ gas sensors. However, because only a limited number of devices were tested, this study does not claim statistical equivalence between the green and chemical silica routes. This demonstrates the feasibility of a circular economy approach where agricultural waste is repurposed into value-added nanomaterials for advanced applications.

- Composite Nanostructure Formation: Both types of silica were effectively integrated with cerium oxide to form $CeO_2$–$SiO_2$ composite nanoparticles. SEM characterization revealed an elongated, rod-like morphology of ceria on a porous silica matrix. The ceria formed elongated, micron-scale rod-like structures, likely composed of intergrown nanoscale $CeO_2$ crystallites rather than isolated particles, indicating strong interactions between $CeO_2$ and the silica template. EDS analysis confirmed a silica-rich composition with cerium present (Si ~42 wt%, Ce ~7 wt%), suggesting a structure where $CeO_2$ is dispersed as a thin layer or clusters on silica. The absence of any foreign elements in EDS and the known chemistry confirm that the composite consisted of $SiO_2$ and $CeO_2$ (with oxygen from both), fulfilling the material design. Although XRD was not performed, the successful sensor performance and literature support imply that the $CeO_2$ is present in its active oxide form.

- Room-Temperature $NH_3$ Sensing Performance: The fabricated silica–ceria sensors showed a strong chemiresistive response to ammonia at room temperature. Upon $NH_3$ exposure, the n-type composite's resistance decreased substantially, yielding a high gas response. Initial exposures produced responses on the order of 600–650% within seconds, highlighting the sensor's high sensitivity and fast kinetics at ambient conditions. This performance is notable since many pure metal oxide sensors require elevated temperatures to reach similar sensitivity. The enhanced response is attributed to the synergy of $CeO_2$'s catalytic redox activity with silica's high surface area and morphological stabilization, which together facilitate efficient $NH_3$ adsorption and reaction at low temperature. We found that the sensor's response was reproducible across both silica sources – indicating that green silica is a viable alternative to chemically synthesized silica in this context, with no observed loss of performance. However, this comparison should be considered preliminary because multiple devices from each synthesis route were not tested statistically. Further work using several sensors, baseline resistance comparison, mean response values, standard deviation, and significance testing is required to confirm whether the green-silica and chemical-silica routes give equivalent sensor performance.

- Time-Dependent Response Evolution: A novel observation in this study is the evolution of the sensor's response over prolonged $NH_3$ exposure (0–15 min). Initially, the sensor's response was positive and large. As exposure continued, the response dynamics became complex, showing peaks, partial recovery, and oscillations, and by 15 minutes the sensor exhibited a negative response (resistance higher in $NH_3$ than in air). We interpret this behavior as a result of surface saturation and prolonged electron donation: essentially, the sensor surface became fully saturated with adsorbates (and oxygen vacancies fully filled), so the normal sensing mechanism (which relies on available $O^-$ species) was impaired. The negative response (~–11%) at 15 min suggests that further $NH_3$ caused additional electron accumulation or a change in surface conduction (possibly through the formation of less-conductive surface compounds), which is consistent with a sensor poisoning or flooding scenario. This finding underscores the importance of considering exposure time in sensor operation – short exposures can be reliably detected with big signals, but continuous exposure can lead to signal rollover or drift. In practical use, either sensors should be regenerated periodically or exposure should be cycled to avoid this saturation. Our work provides a clear example of this phenomenon for ammonia on a ceria-based sensor, complementing prior reports of long-exposure effects in other systems.

- Environmental and Practical Implications: The successful use of bagasse-derived silica in a functional sensor highlights the potential of green nanomaterials in electronic applications. We effectively demonstrated that a waste product can replace a conventionally produced material without sacrificing device performance. This aligns with sustainable development goals by reducing the need for hazardous chemicals and leveraging renewable resources. The sensor developed operates at room temperature, meaning it has low power requirements and is suitable for ambient monitoring (important for safety in agricultural storage, industrial refrigeration, etc., where $NH_3$ leaks are a concern). The high sensitivity observed indicates that even trace levels of $NH_3$ (certainly in the low ppm range or below) should be detectable, though calibration is needed.

- Future Work: To move toward practical deployment, future studies should calibrate the sensor response to known $NH_3$ concentrations and evaluate its selectivity against other gases (such as humidity, which can be a significant interferent for metal-oxide sensors). Long-term stability tests, including cyclic exposures and regeneration techniques, will also be important to address the saturation issue observed. Additionally, incorporating microheaters for periodic high-temperature pulses or UV illumination could help restore the sensor surface after exposure, if continuous operation in $NH_3$ is required. From a materials perspective, exploring different $CeO_2$:$SiO_2$ ratios or doping $CeO_2$ within this composite (e.g., with a catalyst like Pt or a dopant to increase vacancy concentration) might further enhance performance or mitigate saturation. Nonetheless, the core finding remains that integrating green-synthesized silica with ceria yields a high-performance sensor.

In conclusion, this research demonstrates a viable path for green sensor development: using silica from agricultural waste to fabricate a sensitive room-temperature gas sensor. The silica–modified $CeO_2$ composites achieved efficient, rapid detection of ammonia, comparable to sensors made with conventional materials. The study provides insights into sensor behavior under extended exposure, a factor often overlooked, by revealing how response can diminish or invert when the sensor surface becomes saturated. By addressing these insights and limitations, the approach outlined here can be advanced toward robust, eco-friendly gas sensing systems for environmental monitoring and safety applications.

**Acknowledgement. -** During the preparation of this work, the authors used ChatGPT 4.0 to refine writing and improve readability. The authors have reviewed and edited the AI-generated content as necessary and take full responsibility for the contents of this publication.

**References**

[1] A. A. Nayl, A. I. Abd-Elhamid, A. A. Aly, and S. Bräse, "Recent progress in the applications of silica-based nanoparticles," RSC Adv., vol. 12, no. 22, pp. 13706-13726, 2022, https://doi.org/10.1039/D2RA01587K
[2] N. Shafiei, M. Nasrollahzadeh, and S. Iravani, "Green Synthesis of Silica and Silicon Nanoparticles and Their Biomedical and Catalytic Applications," Comments Inorg. Chem., vol. 41, no. 6, pp. 317-372, Nov. 2021, https://doi.org/10.1080/02603594.2021.1904912
[3] N. S. Seroka, R. Taziwa, and L. Khotseng, "Green Synthesis of Crystalline Silica from Sugarcane Bagasse Ash: Physico-Chemical Properties," Nanomaterials, vol. 12, no. 13. p. 2184, 2022. https://doi.org/10.3390/nano12132184
[4] D. Kirubakaran et al., "A Comprehensive Review on the Green Synthesis of Nanoparticles: Advancements in Biomedical and Environmental Applications," Biomed. Mater. Devices, vol. 4, no. 1, pp. 388-413, 2026, https://doi.org/10.1007/s44174-025-00295-4
[5] M. M. Abady, D. M. Mohammed, T. N. Soliman, R. A. Shalaby, and F. A. Sakr, "Sustainable synthesis of nanomaterials using different renewable sources," Bull. Natl. Res. Cent., vol. 49, no. 1, p. 24, 2025, https://doi.org/10.1186/s42269-025-01316-4
[6] D. A. Gkika, K. N. Maroulas, and G. Z. Kyzas, "Various Reduced Graphene Oxide Green Synthetic Routes: Comparing the Cost Procedures," ACS Omega, vol. 10, no. 32, pp. 36221-36237, Aug. 2025, https://doi.org/10.1021/acsomega.5c04090
[7] J. Wang et al., "Enhanced NH3 gas-sensing performance of silica modified CeO2 nanostructure based sensors," Sensors Actuators B Chem., vol. 255, pp. 862-870, 2018, https://doi.org/10.1016/j.snb.2017.08.149
[8] S. Subramanian, K. Neyvasagam, S. Valanarasu, V. Ganesh, I. S. Yahia, and R. Ade, "Room temperature ammonia gas sensor based on Ti-doped CeO2 thin films prepared by nebulizer spray pyrolysis method," Appl. Phys. A, vol. 131, no. 6, p. 457, 2025, https://doi.org/10.1007/s00339-025-08569-w
[9] M. Torkamani Cheriani, A. Mirzaei, and J.-H. Kim, "Resistive-Based Nanostructured CeO2 Gas Sensors: A Review," Chemosensors, vol. 13, no. 8. p. 298, 2025. https://doi.org/10.3390/chemosensors13080298
[10] M. Akbari-Saatlu et al., "Silicon Nanowires for Gas Sensing: A Review," Nanomaterials, vol. 10, no. 11. p. 2215, 2020. https://doi.org/10.3390/nano10112215
[11] M. N. Yaqueen, A. Kuity, and M. A. Ahmed, "Sustainable Nano Silica Production from Agricultural Residues: A Review of Green Synthesis Techniques and Performance in Asphalt Applications," Int. J. Pavement Res. Technol., 2025, https://doi.org/10.1007/s42947-025-00585-6
[12] M. Abdul Sattar, "Circular Economy in Action: Green Synthesis of Mesoporous Silica Nanoparticles from Rice Husk Waste for Biomedical and Industrial Applications," ACS Sustain. Chem. Eng., vol. 13, no. 20, pp. 7617-7630, May 2025, https://doi.org/10.1021/acssuschemeng.5c02582
[13] R. S. Aashikha Shani and A. R. Jeice, "Introspect of prying out silica from agricultural wastes by various methods and incorporating them in distinct uses," Biomass Convers. Biorefinery, vol. 15, no. 4, pp. 5089-5109, 2025, https://doi.org/10.1007/s13399-024-05360-4
[14] I. Kitsou, P. Panagopoulos, T. Maggos, and A. Tsetsekou, "ZnO-coated SiO2 nanocatalyst preparation and its photocatalytic activity over nitric oxides as an alternative material to pure ZnO," Appl. Surf. Sci., vol. 473, pp. 40-48, 2019, https://doi.org/10.1016/j.apsusc.2018.12.146
[15] B.-H. Jang, O. Landau, S.-J. Choi, J. Shin, A. Rothschild, and I.-D. Kim, "Selectivity enhancement of SnO2 nanofiber gas sensors by functionalization with Pt nanocatalysts and manipulation of the operation temperature," Sensors Actuators B Chem., vol. 188, pp. 156-168, 2013, https://doi.org/10.1016/j.snb.2013.07.011
[16] D. E. Newbury* and N. W. M. Ritchie, "Is Scanning Electron Microscopy/Energy Dispersive X-ray Spectrometry (SEM/EDS) Quantitative?," Scanning, vol. 35, no. 3, pp. 141-168, May 2013, https://doi.org/10.1002/sca.21041
[17] H. Mei, F. Zhang, T. Zhou, and T. Zhang, "Pulse-Driven MEMS NO2 Sensors Based on Hierarchical In2O3 Nanostructures for Sensitive and Ultra-Low Power Detection," Sensors, vol. 24, no. 22. p. 7188, 2024. https://doi.org/10.3390/s24227188
[18] M. A. Takte, N. N. Ingle, B. N. Dole, M.-L. Tsai, T. Hianik, and M. D. Shirsat, "A stable and highly-sensitive flexible gas sensor based on Ceria (CeO2) nano-cube decorated rGO nanosheets for selective detection of NO2 at room temperature," Synth. Met., vol. 297, p. 117411, 2023, https://doi.org/10.1016/j.synthmet.2023.117411
[19] D.-H. Gao et al., "Advances in modification of metal and noble metal nanomaterials for metal oxide gas sensors: a review," Rare Met., vol. 44, no. 3, pp. 1443-1496, 2025, https://doi.org/10.1007/s12598-024-03027-7
[20] Z. Tian, J. Li, Z. Zhang, W. Gao, X. Zhou, and Y. Qu, "Highly sensitive and robust peroxidase-like activity of porous nanorods of ceria and their application for breast cancer detection," Biomaterials, vol. 59, pp. 116-124, 2015, https://doi.org/10.1016/j.biomaterials.2015.04.039
[21] X. Tong, W. Shen, X. Chen, and J.-P. Corriou, "A fast response and recovery H2S gas sensor based on free-standing TiO2 nanotube array films prepared by one-step anodization method," Ceram. Int., vol. 43, no. 16, pp. 14200-14209, 2017, https://doi.org/10.1016/j.ceramint.2017.07.165

[22] D. Chen, J. Chen, W. Zhou, and A. Sawut, "Preparation of the New Magnetic Nanoadsorbent Fe3O4@SiO2-yl-VP and Study on the Adsorption Properties of Hg (II) and Pb (II) in Water," Magnetochemistry, vol. 10, no. 12. p. 105, 2024. https://doi.org/10.3390/magnetochemistry10120105
[23] Mallikarjun, K. Gangareddy, and M. V. R. Reddy, "Synthesis of Fe and Cd co-doped CeO2 nanoparticles for highly responsive room temperature ammonia gas sensing application," J. Mater. Sci. Mater. Electron., vol. 35, no. 27, p. 1830, 2024, https://doi.org/10.1007/s10854-024-13591-4
[24] Y. Wang et al., "NH3 gas sensing performance enhanced by Pt-loaded on mesoporous WO3," Sensors Actuators B Chem., vol. 238, pp. 473-481, 2017, https://doi.org/10.1016/j.snb.2016.07.085
[25] Y. Liu et al., "Sulfonic acid-functionalized spiropyran colorimetric gas-sensitive aerogel for real-time visual ammonia sensing," Chem. Eng. J., vol. 511, p. 162160, 2025, https://doi.org/10.1016/j.cej.2025.162160
[26] G. Verma and A. Gupta, "Functional quantum dots: advances and emerging directions for enhanced sensing applications," Nanotechnology, vol. 37, no. 1, p. 12002, 2026, https://doi.org/10.1088/1361-6528/ae2ae3
[27] L. A. September, N. Kheswa, N. S. Seroka, and L. Khotseng, "Green synthesis of amorphous silica nanoparticles (SiO2NPs) from sugarcane bagasse ash by sol-gel method," Next Mater., vol. 10, p. 101396, 2026, https://doi.org/10.1016/j.nxmate.2025.101396
[28] X. He et al., "Polydopamine-coated cerium oxide core-shell nanoparticles for efficient and non-damaging chemical-mechanical polishing," Dalt. Trans., vol. 54, no. 10, pp. 4151-4158, 2025, https://doi.org/10.1039/D4DT03546A
[29] N. Križaj Kosi, J.-S. Pavelić, M. Grilc, S. Gyergyek, and D. Makovec, "Synthesis of a magnetically heatable ceria-supported ruthenium catalyst via deposition of nanocrystalline ceria on silica-coated magnetic iron-oxide nanoparticles," J. Phys. Chem. Solids, vol. 212, p. 113517, 2026, https://doi.org/10.1016/j.jpcs.2026.113517
[30] C. Zhu, D. Li, H. Zhang, D. Zhang, N. Su, and F. Xu, "Effect of montmorillonite-loaded CeO2 nanocomposites with different CeO2 contents on thermal-oxidative and ultraviolet aging properties of asphalt," Constr. Build. Mater., vol. 507, p. 145057, 2026, https://doi.org/10.1016/j.conbuildmat.2025.145057
[31] A. İ. Vaizoğullar, A. Balci, I. Kula, and M. Uğurlu, "Preparation, characterization, and adsorption studies of core@shell SiO2 @ CeO2 nanoparticles: a new candidate to remove Hg (II) from aqueous solutions," Turkish J. Chem., vol. 40, no. 4, pp. 565-575, 2016. https://doi.org/10.3906/kim-1507-7
[32] E. S. Cama, M. Pasini, U. Giovanella, and F. Galeotti, "Crack-Templated Patterns in Thin Films: Fabrication Techniques, Characterization, and Emerging Applications," Coatings, vol. 15, no. 2. p. 189, 2025. https://doi.org/10.3390/coatings15020189
[33] G. Jeerh, "Material and design optimisation of low temperature direct ammonia fuel cells." University of Warwick, 2022.
[34] B. A. Omran, Nanobiotechnology: a multidisciplinary field of science. Springer, 2020. https://doi.org/10.1007/978-3-030-46071-6
[35] J. S. Bates, "Structure and Solvation of Confined Water and Alkanols in Zeolite Acid Catalysis." Purdue University, 2019.
[36] Y. He et al., "Advances in ammonia (NH3) adsorption and storage: materials, mechanisms, and applications," Adsorption, vol. 31, no. 2, p. 48, 2025, https://doi.org/10.1007/s10450-025-00601-y

**Author contribution:**
1. Conception and design of the study
2. Data acquisition
3. Data analysis
4. Discussion of the results
5. Writing of the manuscript
6. Approval of the last version of the manuscript

DM has contributed to: 1, 2, 3, 4, 5 and 6.
SSZZ has contributed to: 1, 2, 3, 4, 5 and 6.
SMM has contributed to: 1, 2, 3, 4, 5 and 6.
MSAA has contributed to: 1, 2, 3, 4, 5 and 6.
AAZ has contributed to: 1, 2, 3, 4, 5 and 6.

**Acceptance Note:** This article was approved by the journal editors Dr. Rafael Sotelo and Mag. Ing. Fernando A. Hernández Gobertti.